Bioconjugate Chemistry

Article

pubs.acs.org/bc

Hydrophobically Modified Keratin Vesicles for GSH-Responsive Intracellular Drug Release

Manuela Curcio,*[,†] Barbara Blanco-Fernandez,[‡] Luis Diaz-Gomez,[‡] Angel Concheiro,[‡] and Carmen Alvarez-Lorenzo[‡]

[†]Department of Pharmacy, Health and Nutritional Sciences, University of Calabria, 87036 Rende (CS), Italy

[‡]Universidad de Santiago de Compostela, Departamento de Farmacia y Tecnología Farmacéutica, Facultad de Farmacia, 15782 Santiago de Compostela, Spain

Supporting Information

ABSTRACT: Redox-responsive polymersomes were prepared by self-assembly of a hydrophobically modified keratin and employing a water addition/solvent evaporation method. Polyethylene glycol-40 stearate ($PEG_{40}ST$) was chosen as hydrophobic block to be coupled to keratin via radical grafting. The amphiphilic polymer exhibited low critical aggregation concentration (CAC; 10 μg/mL), indicating a good thermodynamic stability. The polymeric vesicles loaded both hydrophilic methotrexate and hydrophobic curcumin with high entrapment efficiencies, and showed a GSH-dependent drug release rate. Confocal studies on HeLa cells revealed that the obtained polymersomes were efficiently internalized. Biocompatibility properties of the proposed delivery vehicle were assessed in HET-CAM test and Balb-3T3 mouse fibroblasts. Polymersomes loaded with either methotrexate or curcumin inhibited HeLa and CHO-K1 cancer cells proliferation. Overall, the proposed keratin polymersomes could be efficient nanocarriers for chemotherapeutic agents.

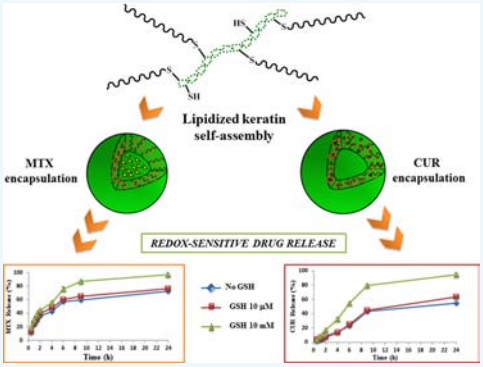

INTRODUCTION

Drug delivery systems able to release their payload in response to disease-related biomarkers are particularly suitable to prevent premature leakage during circulation while efficiently releasing the drug in the affected tissue or cells.[1,2] Glutathione (GSH) concentration gradient between the intracellular (~10 mM) and extracellular (~10 μM) spaces, which strongly modifies the redox potentials across the cellular membrane, is one of the most appealing stimuli. Moreover, GSH concentration in many neoplastic tissues is 4−7-fold higher than that in healthy ones, which is related to cellular proliferation and metastatic activity.[3] These differences in GSH levels make the GSH-responsive nanocarriers very attractive for targeted delivery of anticancer drugs.[4,5].

In parallel, the development of nanocarriers using natural polymers and, in particular, proteins is gaining growing interest due to their low toxicity, abundant renewable sources, and biodegradability, although safety of the degradation products should be ensured.[6] From a technological point of view, proteins may favor emulsifying and gelling processes and their water binding capacity may prevent opsonization by the reticuloendothelial system through an aqueous steric barrier.[7,8]

Furthermore, the abundancy of functional groups in the constituent amino acids allows for tailoring of the physicochemical properties of proteins and their interaction with a great variety of active substances as well as with receptors at cell membranes.[9,10] Some examples of protein-based drug delivery nanovehicles able to respond to the variations of redox environment have already been described. Kommareddy et al.[11] developed poly(ethylene glycol)-modified thiolated gelatin nanoparticles responsive to intracellular GSH concentration for DNA delivery and transfection, and Liu and co-workers[12] reported on the preparation of heterobifunctional protein−polymer conjugates via site-specific modification of albumin with a bifunctional RAFT agent terminated with pyridyl disulfide groups and subsequent in situ polymerization of oligo(ethylene glycol) acrylate and *N*-(2-hydroxypropyl) methacrylamide. In most cases, protein derivatization with sulfide or disulfide group-containing chemical species was needed in order to stabilize the nanoparticles in blood circulation and confer them sufficient GSH-responsive properties. The additional disulfide bonds strengthen the tertiary and quaternary protein structure, and when they are broken, the structure unfolds, releasing the encapsulated payload.

Because of the abundance of cysteine residues (7−20 mol % of all amino acids), keratin (Ker), a biocompatible structural protein[13−16] specialized for hair, wool, feather, nail, and other epithelial coverings, represents a suitable candidate to obtain redox responsive drug delivery systems without chemical modifications of its structure. The cysteine residues are indeed

Received: May 20, 2015
Revised: July 22, 2015
Published: August 19, 2015

DOI: 10.1021/acs.bioconjchem.5b00289
Bioconjugate Chem. 2015, 26, 1900−1907

easily oxidized by air to give inter- and intramolecular disulfide bonds which form the three-dimensional network of keratin fiber,[17] but can be cleaved in the presence of a reducing species such as GSH. In two recent works, polyethylene glycol[18] and poly(*N*-(2-hydroxypropyl)methacrylamide)[19] were attached to Ker backbone via radical grafting, obtaining amphiphilic copolymers able, in water medium, to self-assemble into micelle structures in which Ker constitutes the hydrophobic core. After oxidation of protein thiol groups to disulfide bonds, the nanoparticles behaved as redox-sensitive delivery vehicles of doxorubicin.

Here, on the basis of the previous promising data, Ker was chosen for the first time as base material to synthesize redox-responsive polymersomes. Polymersomes have attracted great attention because of their high stability, tunable membrane properties, versatility, and capacity to transport not only hydrophilic drugs within the aqueous interior compartment, but also hydrophobic drugs within the bilayered membrane.[20,21] The majority of the previously proposed redox-responsive polymersomes have been designed starting from synthetic hydrophilic and hydrophobic blocks.[22,23] So far, GSH-responsive peptide vesicles have been prepared using the amphiphilic oligopeptide SA2 (Ac-Ala-Cys-Val-Cys-Leu-(Leu/Cys)-Leu-Trp-Glu-Glu-COOH) obtained through the introduction of two or three cysteine units able to form intermolecular disulfide bridges into the hydrophobic domain.[24] To the best of our knowledge, the present work represents the first attempt to obtain a GSH-responsive vesicular system based on a natural protein under "green conditions". In the first step, Ker was extracted from wool and hydrophobically modified via radical grafting with polyethylene glycol-40 stearate ($PEG_{40}ST$), a polyoxyl ester widely used in cosmetic and pharmaceutical products.[25,26] Then, self-assembled vesicles, strengthened by the formation of disulfide bonds between the free thiol groups of cysteine in the bilayer structure, were prepared by applying a water addition/solvent evaporation method and characterized regarding shape and size distribution and compatibility against fibroblast cells and chorioallantoic membrane. Due to the amphiphilic nature of the bilayer membrane, the obtained structures may encapsulate both hydrophilic and hydrophobic drugs and release the payload when GSH unfolds the protein by reduction of disulfide groups. Thus, after loading with hydrophilic methotrexate (MTX)[27] and hydrophobic curcumin (CUR)[28] as model molecules, release experiments were performed in reducing media mimicking the GSH concentrations in extra- and intracellular space, while the cytotoxicity and the cellular internalization in CHO-K1 and HeLa tumoral cell lines of the CUR-loaded polymersomes were extensively investigated.

RESULTS AND DISCUSSION

Synthesis and Characterization of Ker-*g*-$PEG_{40}ST$. The abundance of thiol groups easily oxidizable to disulfide bridges makes Ker suitable not only as GSH-responsive component, but also for grafting of polymer chains that can tune its performance. Ker was extracted from wool after reduction of disulfide bonds using thioglycolic acid and urea as reducing agent and protein denaturing agent, respectively. The molecular weight of the resultant hydrolyzed protein, estimated by SDS-PAGE analysis,[29] was in the 15−25 kDa range (Figure 1).

Hydrophobically modified keratin was obtained by preliminary activation of the protein thiol groups by $S_2O_8^{-\cdot}$ radical species, followed by the addition of $PEG_{40}STMA$ to the reaction mixture, as depicted in Figure 2.

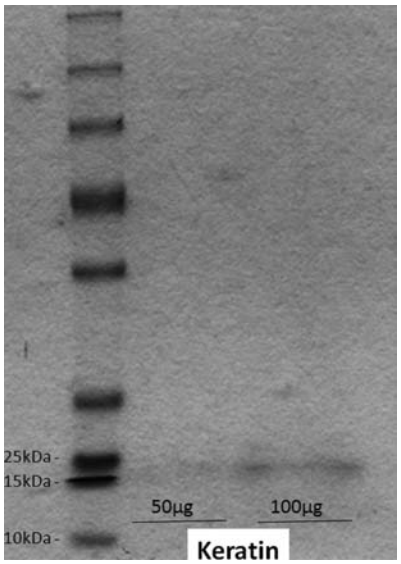

Figure 1. SDS-PAGE analysis of wool-extracted keratin.

$PEG_{40}STMA$ was prepared via trans-esterification of the hydroxyl group of $PEG_{40}ST$ with MA using pyridine as a catalyst. The effective methacrylation was confirmed by FT-IR and ^1H NMR analysis (Figure S1 in Supporting Information). FT-IR spectrum of $PEG_{40}ST$ showed absorption bands at 2975, 1744, and 1210 cm^{-1} due to the stretching vibrations of C—H, C═O, and C−O−C bonds, respectively. $PEG_{40}STMA$ spectrum revealed the appearance of new absorption bands at 1686 and 1626 cm^{-1}, ascribable to the O═C and −C═C− stretching vibrations of methacrylic moiety.

^1H NMR spectrum of $PEG_{40}ST$ showed signals at 0.8 and 1.3 ppm assigned to CH_3 and CH_2 protons of stearic moiety, respectively, and at 3.5−4.0 ppm ascribable to CH_2 protons of PEG. ^1H NMR of $PEG_{40}STMA$ revealed the disappearance of the signal at 4.95 ppm ascribable to the hydroxyl terminal proton, and the presence of two new signals at 5.8 and 6.1 ppm due to the protons of the methacryl groups deriving from the linkage of the methacrylic moiety to $PEG_{40}ST$.

In the conjugation step, the −SH side groups of Ker were activated by $S_2O_8^{-\cdot}$ radical species, and subsequently, $PEG_{40}STMA$ was added obtaining the lipidated protein (Ker-*g*-$PEG_{40}ST$). The grafting of $PEG_{40}ST$ moieties to Ker backbone was confirmed by FT-IR and ^1H NMR analyses (Figure S1 in Supporting Information, spectra 2D). In the ^1H NMR spectrum of Ker-*g*-$PEG_{40}ST$, the peak at δ = 3.5−3.8 ppm ascribable to the protons of oxyethylene moieties of $PEG_{40}ST$ was observed, while in FT-IR two new absorption bands at 2975 and 1210 cm^{-1} ascribable to the stretching vibrations of C−H and C−O−C bonds of $PEG_{40}ST$ were recorded. The substitution degree of Ker-*g*-$PEG_{40}ST$ was estimated by determining the moles of −SH groups in unconjugated and conjugated Ker using Ellman's test, obtaining a value of 27%.

Amphiphilic properties were conferred to Ker by the conjugation with $PEG_{40}ST$ lipid segments, and the resulting conjugate was able to self-assemble in aqueous phase via hydrophobic association of lipid chains.[30] The critical aggregation concentration (CAC) of Ker-*g*-$PEG_{40}ST$ in water was estimated from the dependence of pyrene fluorescence

DOI: 10.1021/acs.bioconjchem.5b00289
Bioconjugate Chem. 2015, 26, 1900−1907

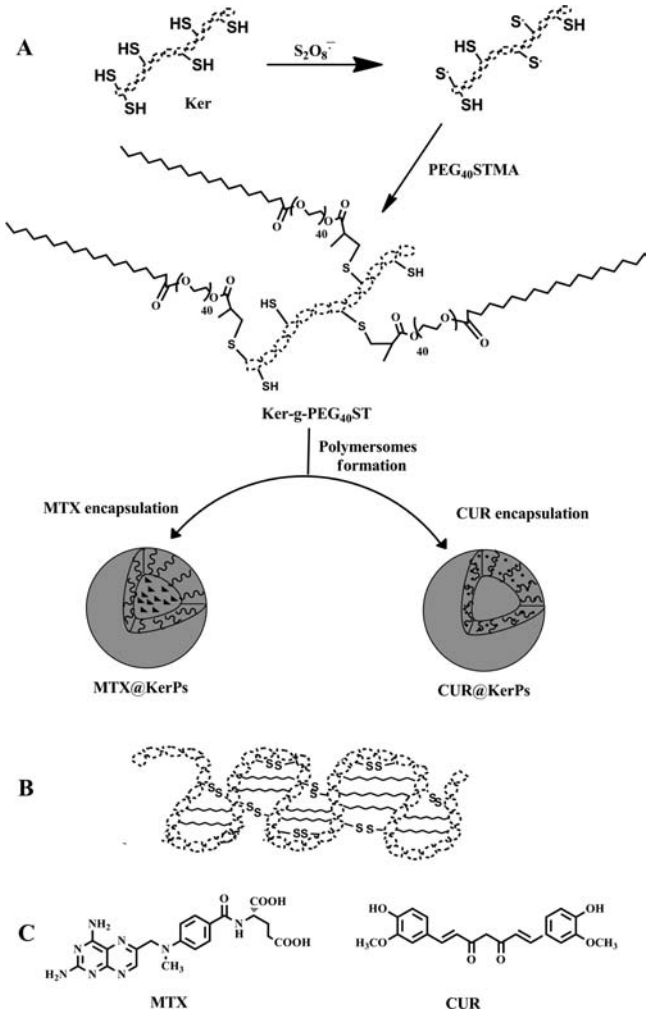

Figure 2. Schematic draws of (A) KerPs formation and subsequent drug loading; (B) hypothesized architecture of the Ker bilayer; and (C) MTX and CUR chemical structures.

spectra (I_{384}/I_{373} ratio) on the conjugate concentration (Figure 3). A sharp change was observed from 10 μg/mL (~0.001% w/w), which was considered to be the CAC. This value is close to the data reported for the previously discussed Ker amphiphilic copolymers[18,19] and indicates that Ker-*g*-PEG_{40}ST aggregates may be stable against dilution.[31] The recorded CAC value is also on the same order of magnitude as that reported for synthetic polypeptide-based copolymers that form vesicular systems.[32−34]

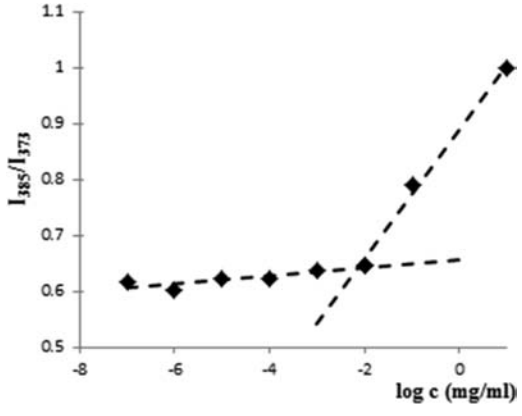

Figure 3. Dependence of pyrene fluorescence spectrum signals on Ker-*g*-PEG_{40}ST concentration.

Synthesis and Characterization of GSH-Responsive KerPs. Glutathione-responsive KerPs were attained by a self-assembly process of Ker-*g*-PEG_{40}ST involving a water addition/solvent evaporation method.[35] In our previous work,[36] a similar procedure was successfully employed to induce the reorganization of hydrophobically modified gelatin hydrolyzates to vesicles structures able to release their payload in a controlled manner. Following this technique, the amphiphilic polymer was dissolved in THF; then, an aqueous phase, consisting of phosphate buffer solution at pH 7.4, was added causing a decrease in solvent quality for the hydrophobic block and leading to polymersome self-assembly. In the last step, the organic solvent was removed by rotary evaporation at 40 °C under reduced pressure. It can be hypothesized that KerPs formation involves the self-assembly of the hydrophobic blocks (mainly stearyl moieties), with the obtainment of vesicles with the hydrophilic portions of Ker and PEG oriented toward the internal and external aqueous environments. The whole structure of the vesicle is further strengthened by in situ cross-linking due to the oxidation of Ker thiol groups to disulfide bonds (Figure 2B).

TEM micrographs of negatively stained KerPs indicated the presence of spherical vesicles (Figure 4); a mean hydrodynamic diameter of 134 nm and a P.D.I. lower than 0.25 were assessed by DLS analysis.

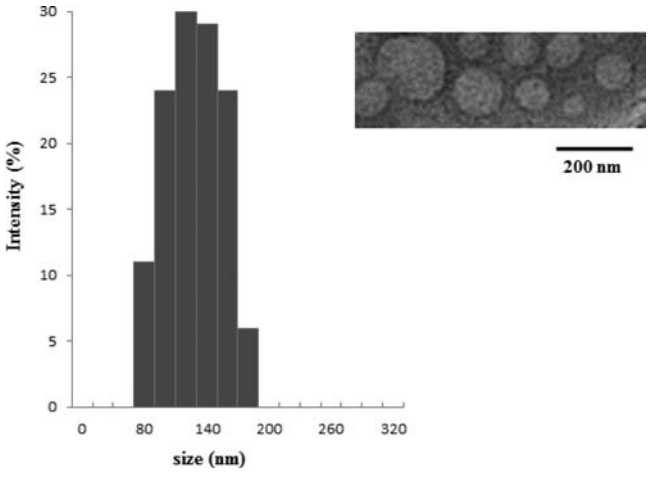

Figure 4. Size distribution obtained from DLS measurements, and TEM image of negatively stained KerPs.

To verify the sensitivity to reducing environments, KerPs were incubated at 37 °C in phosphate buffer containing GSH at different concentrations (0 mM, 10 μM, and 10 mM) for 24 h and then analyzed by DLS. In phosphate buffer without GSH or with 10 μM GSH (concentration in extracellular space) the mean diameter of the KerPs remained almost unchanged, while when the GSH concentration increased to 10 mM (similar to that of the intracellular environment), both the mean diameter and the P.D.I. dramatically increased to 347 nm and 0.34, respectively. This behavior may be ascribable to the breakage of the disulfide bonds induced by the reducing activity of GSH, which destabilizes the microstructure of the bilayer and favors fusion of the vesicles.[22,37,38]

DOI: 10.1021/acs.bioconjchem.5b00289
Bioconjugate Chem. 2015, 26, 1900−1907

Compared to micelles, the main advantage of polymersomes relies on the possibility to encapsulate both hydrophobic (in the lipophilic membrane) and hydrophilic drugs (in the aqueous core).[39] Thus, in separate experiments, CUR and MTX as representatives of hydrophobic and hydrophilic drugs, respectively, were loaded into the obtained vesicles and drug encapsulation was measured by UV−vis spectrophotometry and HPLC, respectively, after dialysis against distilled water. High EE (%) values were recorded for MTX (80%) and CUR (85%), supporting the vesicular structure of the obtained materials. Moreover, DLS measurements of loaded samples demonstrated that, comparing to blank sample, no significant variation in particle size occurred in CUR@KerPs, while the mean diameter of the KerPs raised up to 167 nm following MTX encapsulation. As observed for niosomal bilayers,[40] swelling of polymersomes can be due to the ionization of carboxylic groups of MTX (pK_a 4.8 and 5.5) at pH 7.4, which causes repulsive electrostatic interactions between the negatively charged drug molecules and also with Ker (pI ∼ 4.5).

An ideal stimuli-responsive drug delivery system should not lose any drug during circulation, quickly releasing its payload when targeted tissues or cells are reached.[41] Slow release was recorded for both MTX and CUR in phosphate buffer without GSH or with 10 μM GSH, indicating that the KerPs may be stable in the extracellular medium of healthy tissues and only a small amount of drug would be leaked during blood circulation. Oppositely, when the GSH concentration increased up to 10 mM, a faster release was observed (significant differences; α < 0.05 at all sampling times) due to the breakage of the cross-linking points in the bilayer structure (Figure 5). Moreover,

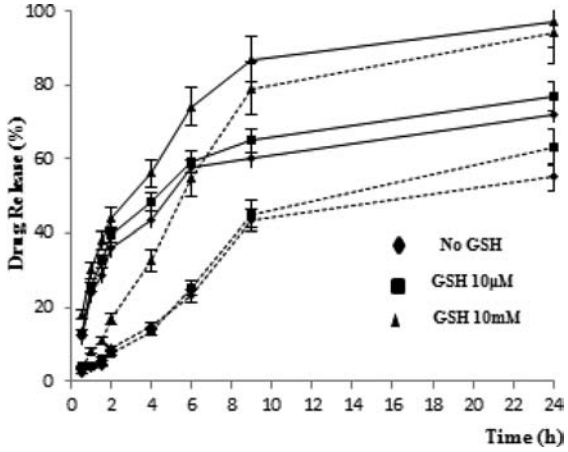

Figure 5. Drug release profiles of MTX (continuous lines) and CUR (dashed lines) from MTX@KerPs and CUR@KerPs, respectively, in phosphate buffer, GSH 10 μM and GSH 10 mM at 37 °C (mean ± standard deviation, n = 3). At every sampling time, percentage of drug released in GSH 10 mM medium was statistically different (α < 0.05) from that recorded in medium without GSH.

compared to MTX, CUR release profiles exhibited minor burst effect and lower release percentages because of the stronger interactions of the hydrophobic drug with the carrier.

Cell Viability Experiments. Cytocompatibility of blank KerPs was assessed by direct contact with Balb3T3 cells for 24 and 48 h. Blank KerPs were tested in the 1.65 to 33 μg/mL concentration range and the results of MTT test proved that cell viability was not compromised at any tested concentration (Figure 6). This means that grafting of $PEG_{40}ST$ does not cause

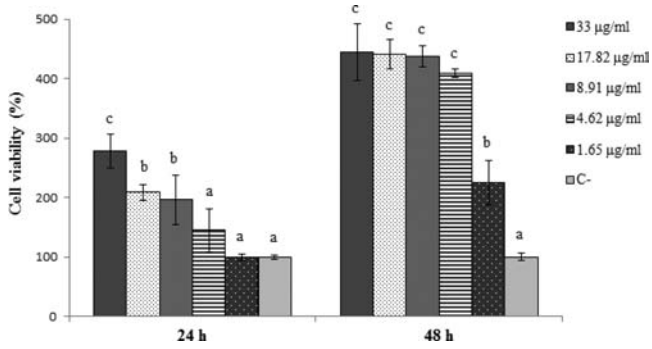

Figure 6. Balb3T3 cell viability after incubation with blank KerPs at different concentrations for 24 or 48 h. Cytocompatibility data were statistically compared (ANOVA α < 0.0001; multiple range test α < 0.05). Equal letter denotes homogeneous groups.

detrimental effects on cytocompatibility of keratin. Cell proliferation observed at high concentrations (significant differences at 24 h $F_{5,12df}$ = 21.76, α < 0.0001, multiple range test α < 0.05; and 48 h $F_{5,12df}$ = 84.05, α < 0.0001, multiple range test α < 0.05) was in accordance with literature demonstrating the high biocompatibility and the positive effect on proliferation of wool and human hair keratin formulations.[13−15,42] In good agreement with these results, concentrated KerPs dispersions (66 μg/mL) did not cause adverse events on the chorioallantoic membrane, which is a non-innervated complete vascularized tissue suitable for irritation tests.[53] The KerPs dispersion did not lead to hemorrhage, lysis, or coagulation, resulting in an IS value of 0 as for the negative control (Figure S2 in Supporting Information). The IS of the positive control was 15.8 ± 0.3.

HeLa (human cervical cancer cell line) and CHO-K1 (a cell line derived from the ovary cancer of the Chinese hamster) were selected as models to evaluate the efficient delivery of MTX and CUR. For MTX@KerPs experiments, folate was not added to the culture media in order to avoid competition between folate and MTX to bind to the dihydrofolate reductase enzyme. MTX is an antagonist of folate and the cytotoxic effect is based on the capability of MTX to prevent the reduction of folic acid to tetrahydrofolate, which is needed for DNA synthesis, cell replication, and protein synthesis.[27] Both MTX@KerPs and CUR@KerPs showed higher cytotoxicity toward HeLa (at 24 h $F_{5,12df}$ = 141.00, α < 0.0001, multiple range test α < 0.05; and 48 h $F_{5,12df}$ = 506.62, α < 0.0001, multiple range test α < 0.05) and CHO-K1 cancer cells (at 24 h $F_{5,12df}$ = 111.33, α < 0.0001, multiple range test α < 0.05; and 48 h $F_{5,12df}$ = 1076.8, α < 0.0001, multiple range test α < 0.05) than free MTX and CUR (Figure 7), suggesting that drug-loaded KerPs could penetrate inside the cells via endocytic processes and release the drug in the cytoplasm where GSH level is higher and the disulfide bonds that integrate polymersomes can be broken, facilitating the drug release (Figure 7).[44,45]

To gain an insight into the uptake of polymersomes by cells, CUR@KerPs were incubated over 2 h with HeLa cells, and then, confocal images were recorded. Compared to MTX, CUR has the advantage of emitting stronger and distinctive fluorescence when observed under confocal microscopy. Cells were also incubated with free CUR dissolved in PBS containing 0.1% Tween 80 in order to check if free CUR could be internalized in the absence of polymersomes. As shown in Figure 8, free CUR was not internalized in HeLa cells, which explains the relatively low cytotoxicity of this drug against

DOI: 10.1021/acs.bioconjchem.5b00289
Bioconjugate Chem. 2015, 26, 1900−1907

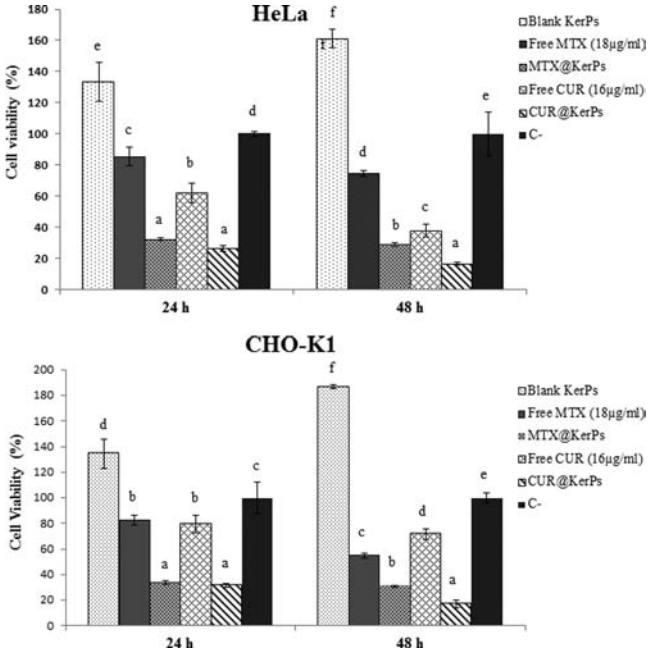

Figure 7. HeLa and CHO-K1 cells viability when exposed to blank and drug-loaded KerPs (33 μg/mL) after 24 and 48 h. Cytocompatibility data were statistically compared (ANOVA $\alpha < 0.0001$; multiple range test $\alpha < 0.05$). Equal letter denotes homogeneous groups.

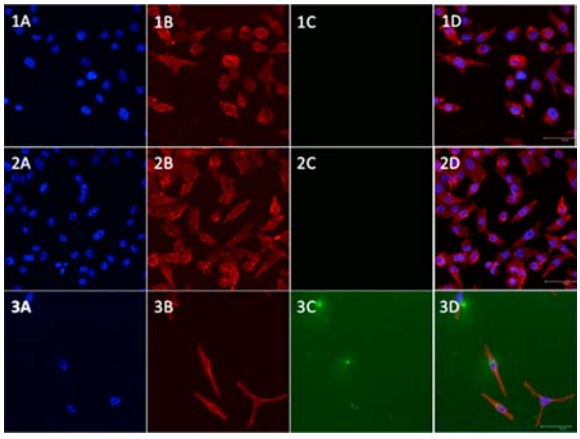

Figure 8. Confocal images (63×) of HeLa cells after incubation over 2 h with culture medium containing Tween 80 (row 1), free CUR dissolved in Tween 80 (row 2), and CUR@KerPs (row 3). Blue channel corresponds to cell nuclei stained with DAPI (A), red channel to cytoskeleton dyed with phalloidin (B), and green channel to CUR (C), and all signals merged (D).

tumoral cells. Conversely, cells incubated with CUR@KerPs presented a high reduction in the cell population and notable morphological changes, associated with a rapid internalization of the nanocarriers and subsequent release of the cytotoxic agent. Moreover, the presence of CUR inside cells incubated with the polymersomes was clearly observed.

CONCLUSIONS

This work reports for the first time on the use of a lipidated natural protein (Ker) for the preparation of redox-responsive vesicles to be employed as nanocarriers for chemotherapeutic drugs. The hydrophobically modified Ker was obtained by means of an eco-friendly approach consisting of covalent conjugation of $PEG_{40}STMA$ to the protein backbone in a fully aqueous medium by radical reaction operating under mild conditions. KerPs showed a spherical shape and a mean diameter of 134 nm and, when placed in media containing a GSH concentration similar to that of intracellular level, exhibited a marked responsiveness. KerPs efficiently encapsulate either hydrophilic (MTX) or hydrophobic (CUR) and exhibited triggerable drug release profiles in media containing an intracellular-like GSH concentration. Studies carried out with HeLa and CHO-K1 cells confirmed the cytotoxic efficiency of the drug-loaded KerPs.

EXPERIMENTAL PROCEDURES

Methodologies. FT-IR spectra were recorded as KBr pellets on a Jasco FT-IR 4200 (Easton, MD, USA). ^{1}H NMR measurements were carried out at 25 °C using DMSO as solvent in a Bruker 500 MHz Advance NMR instrument (Milano, Italy). Pyrene fluorescence emission spectra (λ_{exc} = 336 nm; λ_{em} = 350−500 nm) were recorded on Hitachi F-2500 spectrometer (Brugherio, Italy). Polymersome size distributions were determined using a 90 Plus Particle Size Analyzer DLS instrument (Brookhaven Instruments Corporation, New York, USA) at 25 °C. The autocorrelation function was measured at 90° and the laser beam operated at 658 nm. The polydispersity index (P.D.I.) was directly obtained from the instrumental data fitting procedures by the inverse Laplace transformation and by Contin methods.[46] P.D.I. values ≤0.3 indicate homogeneous and monodisperse populations. Morphological analysis of vesicles was carried out using transmission electron microscopy (TEM; HRTEM/Tecnai F30 [80 kV] FEI company, Hillsboro, OR, USA). A drop of the polymersome dispersion was placed on a Cu TEM grid (200 mesh, Plano GmbH, Wetzlar, Germany), and the sample in excess was removed using a piece of filter paper. A drop of 2% (w/v) phosphotungstic acid solution was then deposited on the carbon grid and left for 2 min. Once the excess staining agent was removed with filter paper, the samples were air-dried and the thin film of stained polymersomes was observed. The quantitative analysis of MTX was performed using a RP-HPLC with Jasco BIP-I pump and Jasco UVDEC-100-V detector. A 250 × 4 mm C-18 Hibar column, 10 μm particle size (Merck, Darmstadt, Germany) was used for the chromatographic separation. The detection wavelength was set at 306 nm. The mobile phase was methanol:0.05% w/w H_3PO_4 (Carlo Erba Reagenti, Milan, Italy) aqueous solution (23/77, v/v) at a flow rate of 1.0 mL min^{-1}.[47] Spectrophotometric analyses were performed using a Jasco V-530 UV/vis spectrometer.

Extraction of Keratin from Wool. Wool fibers from Comisana sheep (Italy) were washed with a mild detergent and cleaned by Soxhlet extraction with petroleum ether to remove fatty matters, thoroughly washed with distilled water, and then dried and cut into short pieces. The pretreated wool (3 g) was mixed with 100 mL of 8 M urea (Carlo Erba Reagenti, Milan, Italy) and 0.2 M thioglycolic acid (Sigma-Aldrich, St. Louis, MO, USA) and adjusted at pH 11 with NaOH 2 M (Carlo Erba Reagenti, Milan, Italy). The mixture was stirred at 50 °C for 24 h, then centrifuged at 12 000 rpm for 5 min in order to eliminate insoluble residues, and filtered. The filtrate was dialyzed for 72 h against deionized water using a dialysis bag with the cutoff molecular weight (MWCO) of 6−8 kDa and replacing the dialyzing medium every 12 h. The molecular weight of the resultant keratin was estimated by SDS-PAGE analysis using a Xcell SureLock Mini-Cell (Life Technologies,

DOI: 10.1021/acs.bioconjchem.5b00289
Bioconjugate Chem. 2015, 26, 1900−1907

Carlsbad, CA, USA), on 12% polyacrylamide gels capable of separating proteins with molecular weights between 188 000 and 3000 Da.[27]

Synthesis of Ker-*g*-PEG$_{40}$ST. Ker-*g*-PEG$_{40}$ST was synthesized following a previously reported procedure[18] with slight changes (synthesis procedure in Supporting Information). The amount of free thiol groups and the substitution degree of the resultant material were determined applying Ellman's assay.[48] Briefly, aliquots (250 μL) of grafted protein aqueous solution (5 mg/mL) were mixed with 0.5 M NaH_2PO_4/Na_2HPO_4 phosphate buffer pH 8.0 (250 μL) and Ellman's reagent (500 μL; 0.3 mg/mL of DTNB in 0.05 M NaH_2PO_4/Na_2HPO_4 phosphate buffer pH 8.0). The reaction was allowed to proceed for 2 h at room temperature and the absorbance was measured at 420 nm. Keratin was used as control and processed in the same way as Ker-*g*-PEG$_{40}$ST. The amount of thiol moieties was calculated from a calibration curve elaborated from solutions of cysteine (0.05 to 0.45 mM) and expressed in terms of millimoles of free sulfhydryl groups per gram of Ker (230 μmol g^{-1}) and Ker-grafted sample (168 μmol g^{-1}).

Determination of the Critical Aggregation Concentration (CAC) of Ker-*g*-PEG$_{40}$ST. The critical aggregation concentration (CAC) of the protein derivative in aqueous phase was determined from fluorescence measurements using pyrene as a nonpolar probe.[49,50] Aliquots (20.0 μL) of pyrene solution (3.0×10^{-5} M, Sigma-Aldrich, St. Louis, MO, USA) in acetone were evaporated in vials. Ker-*g*-PEG$_{40}$ST was dissolved at various concentrations in distilled water under magnetic stirring and then added to the pyrene vials. The contents in the vials were mixed for 12 h, thereby leading to solutions with pyrene concentration of ca. 6.0×10^{-7} M. Then, the intensity ratios (I_3/I_1) of the third vibronic band at 385 nm to the first one at 373 nm of the fluorescence emission spectra of pyrene were recorded at 25 °C.

Preparation of Polymersomes (KerPs). Ker-*g*-PEG$_{40}$ST was dissolved in 10 mL of THF (Carlo Erba Reagenti, Milan, Italy) in a 50 mL round bottomed flask to reach a final concentration 0.1 mg mL^{-1}. Next, 15 mL of phosphate buffer (0.01 M, pH 7.4) were quickly added and vortexed for 2 min at 200 rpm. THF was evaporated using a rotary evaporator (40 rpm, 40 °C, 10 min), yielding the KerPs colloidal system with a final concentration of 0.066 mg mL^{-1}. MTX (Sigma-Aldrich, St. Louis, MO, USA) loaded polymersomes (MTX@KerPs) were prepared as described above, by adding 1 mL of 1.0 mM MTX solution in the phosphate buffer. Similarly, CUR (Sigma-Aldrich, St. Louis, MO, USA) was encapsulated in KerPs (CUR@KerPs) by adding 1 mL of 1.0 mM CUR solution in the Ker-*g*-PEG$_{40}$ST solution in THF.

Entrapment Efficiency. MTX and CUR encapsulation efficiencies (EE%) were determined using the dialysis technique.[51] Briefly, 5 mL of drug loaded KerPs were poured into a dialysis bag (Spectra/Por, MW cutoff 3.5 kDa, Spectrum, Canada) which was immersed in 25 mL of phosphate buffer (154 mM, pH 7.4) for MTX@KerPs, and phosphate buffer (154 mM, pH 7.4) containing 0.1% w/v Tween 80 (Sigma-Aldrich, St. Louis, MO, USA) for CUR@KerPs under magnetic stirring. Tween 80 was added to the medium to provide solubility for CUR in aqueous phase. The dialysis was stopped when no drug was detected in the recipient solution (30 min). Then, 3 mL of purified and nonpurified polymersomes were diluted with 25 mL of methanol (Carlo Erba Reagenti, Milan, Italy), in order to break polymersome membranes, and the MTX and CUR concentrations were measured by HPLC and UV−vis spectrophotometry, respectively.

The entrapment efficiency (EE%) was calculated using the eq 2:

$$\mathrm{EE}(\%) = \frac{\mathrm{ND} - \mathrm{D}}{\mathrm{ND}} \times 100 \tag{2}$$

where ND and D are the drug concentrations before and after the dialysis, respectively.

In Vitro Release Studies. The release experiments were carried out by means of a dialysis method under sink conditions. MTX@KerPs (3 mL) were loaded in a dialysis bag (cutoff molecular weight of 6−8 kDa) and dialyzed against 25 mL of phosphate buffer (154 mM, pH 7.4) containing GSH at different concentrations (0 mM, 10 μM, and 10 mM) at 37 °C in a beaker with constant stirring. At pre-established times, samples (2 mL) of release medium were withdrawn, analyzed using HPLC, and replaced with fresh medium. For CUR@KerPs, drug release was performed under the same conditions but adding 0.1% w/v Tween 80 to the release medium, in order to maintain the sink condition and provide solubility for CUR in aqueous phase.[52] At each experimental time, CUR was determined spectrophotometrically at 450 nm using a standard plot of the drug (0−10 μg/mL) prepared under identical conditions.

HET-CAM Test. The ICCVAM-recommended hen's egg test−chorioallantoic membrane test (HET-CAM) method protocol was followed.[43] In brief, fertilized chicken eggs (Grupo Coren, Galicia, Spain) were incubated at 37 °C and 60% relative humidity (Ineltec CCSP0150 Tona, Barcelona, Spain) for 8 days. The eggshell (air cell) was removed using a rotary saw (Dremel 300, Breda, The Netherlands) and the intact inner membrane of the eggs was moistened with NaCl solution (0.9% w/v) for 30 min. Then, NaCl solution was removed and the inner membrane was carefully removed using forceps. 100 μL of KerPS suspension (66 μg/mL in PBS 154 mM, pH 7.4) were placed on the chorioallantoic membrane and the changes in the vascular tissue exposed to the tested solution were monitored for 5 min. The experiments were carried out in duplicate. 0.9% NaCl solution and 0.1 N NaOH were used as negative and positive control, respectively. Irritation scores (IS) were calculated from the time in seconds at which hemorrhage (H), lysis (L), or coagulation (C) started, as follows:

$$\mathrm{IS} = \left(\frac{301 - H_{\mathrm{time}}}{300}\right) \times 5 + \left(\frac{301 - L_{\mathrm{time}}}{300}\right) \times 7 + \left(\frac{301 - C_{\mathrm{time}}}{300}\right) \times 9$$

Cell Culture and Cell Growth Inhibition Assays. BALB/3T3 (ATCC CCL-163), CHO-K1 (ATCC CCL-61), and HeLa (ATCC CCL-2) cells in RPMI 1640, supplemented with 10% FBS and 1% antibiotic solution (10 000 units/mL penicillin/ and 10 000 μg/mL streptomycin), were seeded in 96-well plates (100 μL, 200 000 cells/mL) and incubated for 12 h at 37 °C, 5% CO_2, and 90% RH. For MTX experiments, RPMI medium without folic acid was used in order to avoid competitive interactions between MTX and the folic acid of the medium. Afterward, for BALB/3T3 experiments 100 μL of blank KerPs suspensions freshly prepared at different concentrations (1.7; 4.6; 9.0; 18.0; 33.0 μg KerPs/mL) in culture medium were added to the wells containing cells. For

DOI: 10.1021/acs.bioconjchem.5b00289
Bioconjugate Chem. 2015, 26, 1900−1907

the experiments with cancer cells, 100 μL of blank or drug-loaded KerPs dispersions freshly prepared (33.0 μg KerPs/mL in culture medium) were added to the wells containing cells. MTX and CUR solutions (200 μL; 20 μg/mL for both MTX and CUR) were used as positive controls. Cells cultured in fresh medium were used as negative control. After 24 and 48 h of incubation, the medium was replaced with 100 μL of fresh medium, and the cytocompatibility was measured following the instructions of the MTT kit (Roche, Switzerland). The absorbance was measured at 550 nm using an ELISA plate reader (BIORAD model 680 Microplate Reader, USA). All experiments were carried out in triplicate.

Cell Uptake Experiments. HeLa cells were seeded in 8-well glass slides (50 000 cells/well, Millicell EZ slides, Millipore) and incubated for 24h (37 °C, 5% CO_2). Then, cells were washed with PBS, and CUR@KerPs dispersed in RPMI medium (KerPs concentration 33 μg/mL) were added. A positive control with curcumin (16 μg/mL) dissolved in 0.1% Tween 80 and a negative control with PBS were also carried out. After 2 h in culture, medium was removed and wells were washed with PBS. Subsequently, cells were fixed with paraformaldehyde 4% (100 μL, 10 min), washed three times with PBS, incubated with Triton X-100 (0.2% in PBS pH 7.4, 40 μL, 5 min), and washed again three times with PBS. Then, cellular cytoskeleton (F-actin) staining was carried out using phalloidin dye (BODIPY 650/665 phalloidin; Molecular Probes by Life Technologies, Eugene, OR, USA) (40 μL, 75 nM in PBS, 20 min) and washed again three times with PBS. Afterward, one drop of ProLong gold antifade reagent (Molecular Probes by Life Technologies, Eugene, OR, USA) was added to each sample, covered with a cover glass, and kept frozen until analysis. Confocal images were recorded using a Leica confocal TCS-SP2 (Leica Microsystems, Wetzlar, Germany) and processed with LAS AF software (Leica Microsystems, Wetzlar, Germany).

Statistical Analysis. Drug release percentage at each time in the different media and cytocompatibility values recorded for KerPs formulations were analyzed using ANOVA and multiple range test (Statgraphics Centurion XVI 1.15, StatPoint Technologies Inc., Warranton VA).

■ ASSOCIATED CONTENT

Supporting Information

The Supporting Information is available free of charge on the ACS Publications website at DOI: 10.1021/acs.bioconjchem.5b00289.

Synthesis of $PEG_{40}STMA$; Synthesis of Ker-*g*-$PEG_{40}ST$; FT-IR and ^1H NMR results of $PEG_{40}ST$, $PEG_{40}STMA$, Ker and Ker-*g*-$PEG_{40}ST$; HET-CAM results of KerPs dispersion (PDF)

■ AUTHOR INFORMATION

Corresponding Author

*E-mail: manuela.curcio@unical.it. Tel/Fax: +39 0984 493011.

Notes

The authors declare no competing financial interest.

■ REFERENCES

(1) Sun, Q., Radosz, M., and Shen, Y. (2012) Challenges in design of translational nanocarriers. *J. Controlled Release 164*, 156−169.

(2) Alvarez-Lorenzo, C., and Concheiro, A. (2014) Smart drug delivery systems: from fundamentals to the clinic. *Chem. Commun. 50*, 7743−7765.

(3) Traverso, N., Ricciarelli, R., Nitti, M., Marengo, B., Furfaro, A. L., Pronzato, M. A., Marinari, U. M., and Domenicotti, C. (2013) Role of glutathione in cancer progression and chemoresistance. *Oxid. Med. Cell. Longevity 2013*, 1.

(4) Saito, G., Swanson, J. A., and Lee, K. D. (2003) Drug delivery strategy utilizing conjugation via reversible disulfide linkages: role and site of cellular reducing activities. *Adv. Drug Delivery Rev. 55*, 199−215.

(5) Meng, F., Hennink, W. E., and Zhong, Z. (2009) Reduction-sensitive polymers and bioconjugates for biomedical applications. *Biomaterials 30*, 2180−2198.

(6) Elzoghby, A. O., Samy, W. M., and Elgindy, N. A. (2012) Protein-based nanocarriers as promising drug and gene delivery systems. *J. Controlled Release 161*, 38−46.

(7) Elzoghby, A. O., Abo El-Fotoh, W. S., and Elgindy, N. A. (2011) Casein-based formulations as promising controlled release drug delivery systems. *J. Controlled Release 153*, 206−216.

(8) Elzoghby, A. O., Samy, W. M., and Elgindy, N. A. (2012) Albumin-based nanoparticles as potential controlled release drug delivery systems. *J. Controlled Release 157*, 168−182.

(9) Curcio, M., Spizzirri, U. G., Iemma, F., Puoci, F., Cirillo, G., Parisi, O. I., and Picci, N. (2010) Grafted thermo-responsive gelatin microspheres as delivery systems in triggered drug release. *Eur. J. Pharm. Biopharm. 76*, 48−55.

(10) MaHam, A., Tang, Z., Wu, H., Wang, J., and Lin, Y. (2009) Protein-based nanomedicine platforms for drug delivery. *Small 5*, 1706−1721.

(11) Kommareddy, S., and Amiji, M. (2005) Preparation and evaluation of thiol-modified gelatin nanoparticles for intracellular DNA delivery in response to glutathione. *Bioconjugate Chem. 16*, 1423−1432.

(12) Liu, J. Q., Liu, H. Y., Bulmus, V., Tao, L., Boyer, C., and Davis, T. P. (2010) A simple methodology for the synthesis of heterotelechelic protein-polymer-biomolecule conjugates. *J. Polym. Sci., Part A: Polym. Chem. 48*, 1399−1405.

(13) Yamauchi, K., Maniwa, M., and Mori, T. (1998) Cultivation of fibroblast cells on keratin-coated substrata. *J. Biomater. Sci., Polym. Ed. 9*, 259−270.

(14) Wang, S., Taraballi, F., Tan, L. P., and Ng, W. K. (2012) Human keratin hydrogels support fibroblast attachment and proliferation in vitro. *Cell Tissue Res. 347*, 795−802.

(15) Reichl, S. (2009) Films based on human hair keratin as substrates for cell culture and tissue engineering. *Biomaterials 30*, 6854−6866.

(16) Rouse, J. G., and Van Dyke, M. E. (2010) A review of keratin-based biomaterials for biomedical applications. *Materials 3*, 999−1014.

(17) Katoh, K., Shibayama, M., Tanabe, T., and Yamauchi, K. (2004) Preparation and physicochemical properties of compression-molded keratin films. *Biomaterials 25*, 2265−2272.

(18) Li, Q., Zhu, L., Liu, R., Huang, D., Jin, X., Che, N., Li, Z., Qu, X., Kang, H., and Huang, Y. (2012) Biological stimuli responsive drug carriers based on keratin for triggerable drug delivery. *J. Mater. Chem. 22*, 19964−19973.

(19) Li, Q. M., Yang, S. N., Zhu, L. J., Kang, H. L., Qu, X. Z., Liu, R. G., and Huang, Y. (2015) Dual stimuli sensitive keratin graft PHPMA as physiological trigger responsive drug carriers. *Polym. Chem. 6*, 2869−2878.

(20) Messager, L., Gaitzsch, J., Chierico, L., and Battaglia, G. (2014) Novel aspects of encapsulation and delivery using polymersomes. *Curr. Opin. Pharmacol. 18*, 104−111.

(21) Discher, D. E., and Eisenberg, A. (2002) Polymer vesicles. *Science 297*, 967−973.

(22) Ren, T., Wu, W., Jia, M., Dong, H., Li, Y., and Ou, Z. (2013) Reduction-Cleavable Polymeric Vesicles with efficient glutathione-mediated drug release behavior for reversing drug resistance. *ACS Appl. Mater. Interfaces 5*, 10721−10730.

DOI: 10.1021/acs.bioconjchem.5b00289
Bioconjugate Chem. 2015, 26, 1900−1907

(23) Xu, H. F., Meng, F. H., and Zhong, Z. Y. (2009) Reversibly crosslinked temperature-responsive nano-sized polymersomes: synthesis and triggered drug release. *J. Mater. Chem. 19*, 4183−4190.
(24) Van Hell, A. J., Crommelin, D. J. A., Hennink, W. E., and Mastrobattista, E. (2009) Stabilization of peptide vesicles by introducing inter-peptide disulfide bonds. *Pharm. Res. 26*, 2186−2193.
(25) Zhu, S., Huang, R., Hong, M., Jiang, Y., Hu, Z., Liu, C., and Pei, Y. (2009) Effects of polyoxyethylene (40) stearate on the activity of P-glycoprotein and cytochrome P450. *Eur. J. Pharm. Sci. 37*, 573−580.
(26) Luo, L., Xu, X., Shi, B., Wu, J., and Hu, Y. (2007) Polyoxyethylene 40 stearate modulates multidrug resistance and enhances antitumor activity of vinblastine sulfate. *AAPS J. 9*, E329−E335.
(27) Tian, H., and Cronstein, B. N. (2007) Understanding the mechanisms of action of methotrexate: implications for the treatment of rheumatoid arthritis. *Bull. NYU Hosp. Jt. Dis. 65*, 168−173.
(28) Baell, J., and Walters, M. A. (2014) Chemical con artists foil drug discovery. *Nature 513*, 481−483.
(29) Zoccola, M., Aluigi, A., and Tonin, C. (2009) Characterisation of keratin biomass from butchery and wool industry wastes. *J. Mol. Struct. 938*, 35−40.
(30) Chiang, W. H., Lan, Y. J., Huang, Y. C., Chen, Y. W., Huang, Y. F., Lin, S. C., Chern, C. S., and Chiu, H. C. (2012) Multi-scaled polymersomes from self-assembly of octadecanol-modified dextrans. *Polymer 53*, 2233−2244.
(31) Huang, Z., Teng, W., Liu, L., Wang, L., Wang, Q., and Dong, Y. (2013) Efficient cytosolic delivery mediated by polymersomes facilely prepared from a degradable, amphiphilic, and amphoteric copolymer. *Nanotechnology 24*, 265104.
(32) Zhao, L., Li, N., Wang, K., Shi, C., Zhang, L., and Luan, Y. (2014) A review of polypeptide-based polymersomes. *Biomaterials 35*, 1284−1301.
(33) Quadir, M. A., Morton, S. W., Deng, Z. J., Shopsowitz, K. E., Murphy, R. P., Epps, T. H., and Hammond, P. T. (2014) PEG-polypeptide block copolymers as pH-responsive endosome-solubilizing drug nanocarriers. *Mol. Pharmaceutics 11*, 2420−2430.
(34) Chen, P., Qiu, M., Deng, C., Meng, F., Zhang, J., Cheng, R., and Zhong, Z. (2015) pH-responsive chimaeric pepsomes based on asymmetric poly(ethylene glycol)-b-poly(L-leucine)-b-poly(L-glutamic acid) triblock copolymer for efficient loading and active intracellular delivery of doxorubicin hydrochloride. *Biomacromolecules 16*, 1322−1330.
(35) Marsden, H. R., Gabrielli, L., and Kros, A. (2010) Rapid preparation of polymersomes by a water addition/solvent evaporation method. *Polym. Chem. 1*, 1512−1518.
(36) Curcio, M., Cirillo, G., Vittorio, O., Spizzirri, U. G., Iemma, F., and Picci, N. (2015) Hydrolyzed gelatin-based polymersomes as delivery devices of anticancer drugs. *Eur. Polym. J. 67*, 304−313.
(37) Lin, C., Zhong, Z., Lok, M. C., Jiang, X., Hennink, W. E., Feijen, J., and Engbersen, J. F. J. (2007) Novel bioreducible poly(amido amine)s for highly efficient gene delivery. *Bioconjugate Chem. 18*, 138−145.
(38) Li, Y., Lokitz, B. S., Armes, S. P., and McCormick, C. L. (2006) Synthesis of reversible shell cross-linked micelles for controlled release of bioactive agents. *Macromolecules 39*, 2726−2728.
(39) Colley, H. E., Hearnden, V., Avila-Olias, M., Cecchin, D., Canton, I., Madsen, J., MacNeil, S., Warren, N., Hu, K., McKeating, J. A., Armes, S. A., Murdoch, C., Thornhill, M. H., and Battaglia, G. (2014) Polymersome-mediated delivery of combination anticancer therapy to head and neck cancer cells: 2D and 3D in vitro evaluation. *Mol. Pharmaceutics 11*, 1176−1188.
(40) Muzzalupo, R., Tavano, L., and La Mesa, C. (2013) Alkyl glucopyranoside-based niosomes containing methotrexate for pharmaceutical applications: Evaluation of physico-chemical and biological properties. *Int. J. Pharm. 458*, 224−229.
(41) Sun, H., Meng, F., Cheng, R., Deng, C., and Zhong, Z. (2014) Reduction and pH dual-bioresponsive crosslinked polymersomes for efficient intracellular delivery of proteins and potent induction of cancer cell apoptosis. *Acta Biomater. 10*, 2159−2168.
(42) Yamauchi, K., Maniwa, M., and Mori, T. (1998) Cultivation of fibroblast cells on keratin-coated substrata. *J. Biomater. Sci., Polym. Ed. 9*, 259−270.
(43) NICEATM-ICCVAM, In vivo Test Methods for Detecting Ocular Corrosives and Severe Irritants, http://ntp.niehs.nih.gov/iccvam/docs/ocutox_docs/oteval/appg-508.pdf (accessed July 2015).
(44) Thambi, T., Deepagan, V. G., Ko, H., Lee, D. S., and Park, J. H. (2012) Bioreducible polymersomes for intracellular dual-drug delivery. *J. Mater. Chem. 22*, 22028−22036.
(45) Ren, T., Wu, W., Jia, M., Dong, H., Li, Y., and Ou, Z. (2013) Reduction-cleavable polymeric vesicles with efficient glutathione-mediated drug release behavior for reversing drug resistance. *ACS Appl. Mater. Interfaces 5*, 10721−10730.
(46) Provencher, S. W. (1982) Constrained regularization method for inverting data represented by linear algebraic or integral equation. *Comput. Phys. Commun. 27*, 213−227.
(47) Liu, X., Liu, J., Huang, Y., Zhao, R., Liu, G., and Chen, Y. (2009) Determination of methotrexate in human serum by high-performance liquid chromatography combined with pseudo template molecularly imprinted polymer. *J. Chromatogr. A 1216*, 7533−7538.
(48) Anitha, A., Deepa, N., Chennazhi, K. P., Nair, S. V., Tamura, H., and Jayakumar, R. (2011) Development of mucoadhesive thiolated chitosan nanoparticles for biomedical applications. *Carbohydr. Polym. 83*, 66−73.
(49) Besheer, A., Hause, G., Kressler, J., and Mäder, K. (2007) Hydrophobically modified hydroxyethyl starch: synthesis, characterization, and aqueous self-assembly into nano-sized polymeric micelles and vesicles. *Biomacromolecules 8*, 359−367.
(50) Hu, X. L., Liu, S., Chen, X. S., Mo, G. J., Xie, Z. G., and Jing, X. B. (2008) Biodegradable amphiphilic block copolymers bearing protected hydroxyl groups: synthesis and characterization. *Biomacromolecules 9*, 553−560.
(51) Tavano, L., Muzzalupo, R., Trombino, S., Cassano, R., Pingitore, A., and Picci, N. (2010) Effect of formulations variables on the in vitro percutaneous permeation of sodium diclofenac from new vesicular systems obtained from Pluronic triblock copolymers. *Colloids Surf., B 79*, 227−234.
(52) Yallapu, M. M., Gupta, B. K., Jaggi, M., and Chauhan, S. C. (2010) Fabrication of curcumin encapsulated PLGA nanoparticles for improved therapeutic effects in metastatic cancer cells. *J. Colloid Interface Sci. 351*, 19−29.
(53) Scheel, J., Kleber, M., Kreutz, J., Lehringer, E., Mehling, A., Reisinger, K., and Steiling, W. (2011) Eye irritation potential: usefulness of the HET-CAM under the globally harmonized system of classification and labeling of chemicals (GHS). *Regul. Toxicol. Pharmacol. 59*, 471−492.

DOI: 10.1021/acs.bioconjchem.5b00289
Bioconjugate Chem. 2015, 26, 1900−1907